Arch. Metall. Mater. **69** (2024), 3, 1143-1149

DOI: https://doi.org/10.24425/amm.2024.150936

M. BRŮNA[1], M. GALČÍK[1*], M. MEDŇANSKÝ[1], J. KASIŃSKA[2]

UNCONVENTIONAL ELEMENTS IN THE GATING SYSTEM AND THEIR INFLUENCE ON THE MELT FLOW AND CASTING QUALITY

The naturally pressurized gating system appears to be an appropriate solution for reoxidation reduction, but this type of gating system can result in supercritical melt velocity. The paper is focused on the determination of the unconventional elements effect in the gating system on the melt velocity and melt flow and their influence on the mechanical properties and microstructure. In experimental works was observed the influence of dimensioned gate, foam filters with 10 and 30 ppi density, trident gate and combination of trident gate and vortex element. Melt velocity was observed by simulation software and via velocity measurement by contact method in the mold during casting. Melt flow was analyzed by simulation software and water model experiment. Experimental casts have been made for the purpose of evaluating mechanical properties and microstructure determination. The best results were achieved by 30 ppi foam filter.

Keywords: Melt velocity; melt flow; gating system; unconventional elements; casting quality

1. Introduction

Increasing ecological requirements are connected to enlarging production of aluminium alloys because they are able to achieve a good ratio between mechanical properties and density [1-4]. It leads to increasing demands on the quality of castings. It is therefore important to remove as many defects as possible from the castings. And thus, it is necessary to know the mechanism of defects in castings. One of the main problems affecting the final quality of aluminium alloy castings is the reoxidation processes. It occurs during filling of the gating system and the mold cavity. A thin oxide layer is almost immediately formed on the surface of the aluminium alloy melt when it is in contact with the surrounding atmosphere. The problem arise when the turbulence of the melt surface leads to the entrainment of the surface oxide layers into the melt volume and double oxide layers are formed. Entrained double oxide layers can pass through the entire gating system and solidify in the casting, which can significantly reduce its quality. One of the main parameters influencing the formation of double oxide layers is the melt velocity [5-9].

Achieving increased casting quality is connected to reduce the rate of reoxidation processes in the gating system during filling. It was shown that reoxidation processes can be positively influenced by a suitable design of the gating system [6,10-12]. The aim is to replace the commonly used non-pressurised gating system for casting aluminium alloys by a naturally pressurized gating system. In practice, this replacement of the gating system is not yet well accepted because of the lack of more extensive knowledge. The main reason is the critical melt velocity occurring at the end of the gating system. Therefore, a suitable solution to reduce it needs to be found. In the works [6,13-15] was melt velocity reduced by foundry filters placed in the runner or in the gates. Beneficial effect of vortex gate and vortex element was analysed in research [12,14,16,17]. Trident gate seem to be also suitable for melt velocity reduction and melt flow improvement in the mold cavity, which was observed in works [12,17].

In this work, naturally pressurized gating system was designed and analysed a comprehensive overview of dimensioned gate, foam filters, trident gate and trident gate with bubble trap effect on melt velocity, melt flow, mechanical properties and microstructure. Effectiveness of these elements on the melt velocity was observed during filling of the mold by real melt velocity measurement and by simulation software. For determination of their influence on melt flow in the mold cavity was suggested experiment with inspection fluid and simulation analysis. After experimental casts, used elements influence on the mechanical properties and microstructure was determined.

[1] UNIVERSITY OF ŽILINA, FACULTY OF MECHANICAL ENGINEERING, UNIVERZITNÁ 8215/1, 010 26 ŽILINA, SLOVAK REPUBLIC
[2] KIELCE UNIVERSITY OF TECHNOLOGY, FACULTY OF MECHATRONICS AND MECHANICAL ENGINEERING, 7 TYSIĄCLECIA PAŃSTWA POLSKIEGO AV., 25-314 KIELCE, POLAND
* Corresponding author: marek.galcik@fstroj.uniza.sk

2. Materials and methods

For experimental purposes of this work naturally pressurized gating system was designed. Dimensions of used foam filters were 50×50×20 mm. In order to compare the influence of the used elements, a gating system without filter and with gate of the same cross-section dimensions as a runner (Design 1) was used as a reference gating system (Fig. 1a). Another design is the gating system with a dimensioned gate (Design 2) as shown in Fig. 1b. The area of this gate has been determined by calculation according to work [5] so that the melt velocity at this location is a maximum of 0.5 $m.s^{-1}$. Fig. 1c shows a design in which a 10 ppi foam filter (Design 3) and a 30 ppi foam filter (Design 4) were placed in the gate area horizontally above the runner. In another design (Fig. 1d), the influence of a trident gate (Design 5) was evaluated. This type of gate consists of bubble trap and chambers for two filters. One filter is placed horizontally above the runner and the placement of the second filter is vertical. Foam filters with a density of 20 ppi were inserted into the chambers. The output gate area in the trident gate remains unchanged from the gate area calculation in Design 1. In the last design (Fig. 1e), a combination of a trident gate with two 20 ppi foam filters and a cylindrical-shaped vortex element at the end of the runner was used (Design 6) and offset pouring basin was used in all designs.

Aluminium alloy AlCu4Ti was used for casting without any modification, grain refinement and degassing. This alloy was chosen because it is widely used in our region which is focused on automotive industry. The chemical composition of the castings is shown in the TABLE 1 as average value of three measurements. The chemical composition was measured on a Q2 ION spectrometer. The casting process conditions are shown in the TABLE 2. Basic boundary numerical simulation conditions were set to that the casting temperature was 745°C, initial temperature was 20°C, resin bonded sand molds were used and casted alloy was EN AC-21000 AlCu4MgTi. An electric resistance furnace was used for melting process and the melt temperature was controlled using "K" type thermocouples. After casting process, the specimens intended to mechanical properties evaluation was heat treated. Heat treatment conditions was T6 (annealing temperature 525 ± 5°C, annealing time 14 hours, water temperature 35 °C, artificial aging temperature 155 ± 5°C, aging time 8 hours).

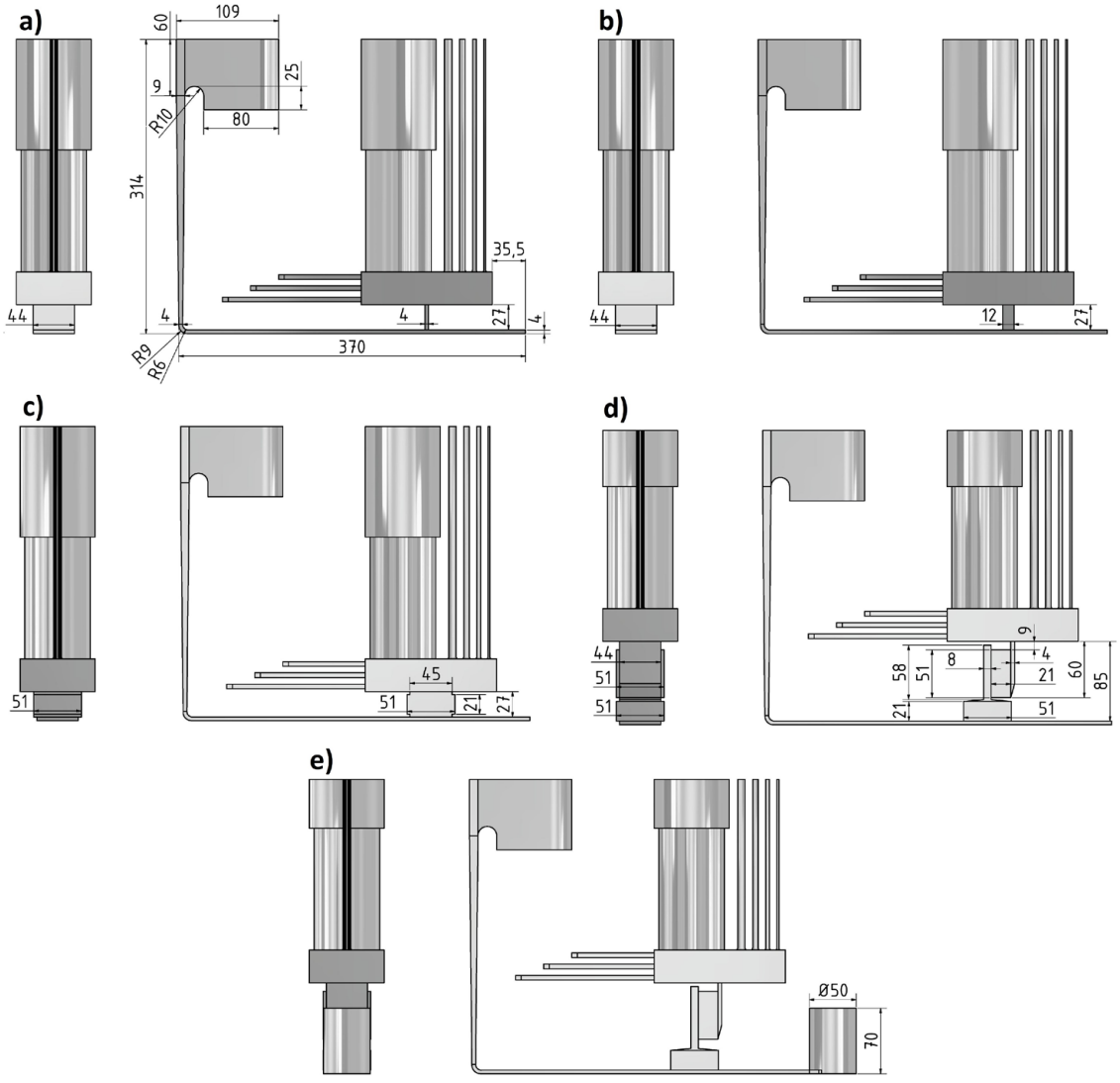

Fig. 1. Deign of gating system: a) Design 1, b) Design 2, c) Design 3 and Design 4, d) Design 5, e) Design 6

TABLE 1

Chemical composition of AlCu4Ti

Element	Si	Fe	Cu	Mn	Zn	Ti	Al
w.%	0,05	0,11	5,03	0,42	0,01	0,19	bal.

TABLE 2

Pouring conditions

Casting temperature	745 ± 5°C
Mold and ambient temperature	17 ± 2°C
Casting height	100 mm
Melt level in the pouring basin	30 mm
Casting method	gravity
Mold type	sand

The molds consisted of two sand blocks (dimensions 500×350×75 mm) of silica sand and phenol formaldehyde resin. After mixing of sand and resin it was cured using CO_2. Designs 1-6 were milled on CNC milled machine into the sand blocks by a patternless process method. A graphite coating was applied to the machined surface, melt velocity measuring sensors were fitted to the molds and foam filters were inserted. The individual mold preparation steps are shown in Fig. 2.

The melt velocity was evaluated using sensors during casting and via the ProCAST simulation software. The melt flow in the mold cavity was observed using simulations and by experiment with inspection fluid. The casting process was followed by evaluation of mechanical properties (ultimate strength, conventional yield strength, ductility, notch toughness) and microstructural analysis.

3. Results and discussion

3.1. Melt velocity

Melt velocity is a significant factor during filling the mold cavity, therefore, direct measurement of melt velocity during casting was applied using sensors and the values were compared with the results from the simulation analysis.

The sensors RE, E1, E2, E3 and E4 were located in the mold and their placement location during casting is shown in Fig. 3. In all gating system designs, sensors RE, E1, and E2 were placed in the runner and the E4 sensors were located after the gates location. Placement of E3 sensors were in the gates. The RE, E1 and E3 sensors performed only an auxiliary function and no velocity was measured at these locations. Melt velocity was only measured via sensors E2 and E4. Sensors E2 were placed in the runner before gates and E4 sensors after gates. The melt velocity measurements at these locations were chosen to evaluate the effectiveness of the used gating system design elements on the melt velocity entering the mold cavity. Sensors were 1.4 mm diameter copper wires connected to a NATIONAL INSTRUMETNS NI USB-6008 measurement module which was connected to a computer. The measurement methodology was based on the fact, that a voltage was applied to the first sensor RE from a stabilized laboratory source, when the melt was in contact with sensor E1, between sensors RE and E1 was created electrical circuit and a voltage rise was observed at that sensor E1 at the time of contact with the melt. When the melt is in the contact with sensor E2, the closed electrical circuit between the sensors E1 and E2 was again formed, and a voltage increased. At the other sensors the measurement was carried out in the same way. In each mold, the distance between the sensors was measured. The distance between each sensors and the time it took the melt to travel that distance was known. Average melt velocity was calculated from the difference in the distance between sensors and the peaks of voltage reached in time on the sensors. Time and voltage data for sensors E1 to E4 were recorded using software LabVIEW 2020.

The first melt velocity was measured at E2. Without automatic casting, it is not possible to maintain identical casting conditions for all designs, but the melt velocity values at point E2 shown that the filling conditions were approximately the same in all designs. Range of the melt velocity at this point was from 0.81 to 0.91 $m.s^{-1}$. The second melt velocity measurement point was sensor E4 located in each mold approximately 5 mm after gate location. The results shown a decrease in melt velocity at this point in Designs 2 to 5 compared to the reference gating system. In Design 6, the melt velocity could not be evaluated at

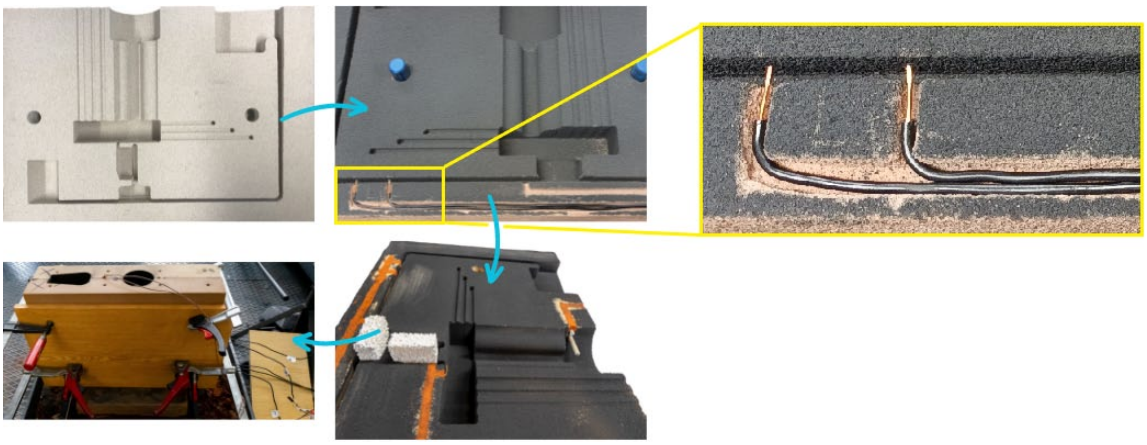

Fig. 2. Mold preparation

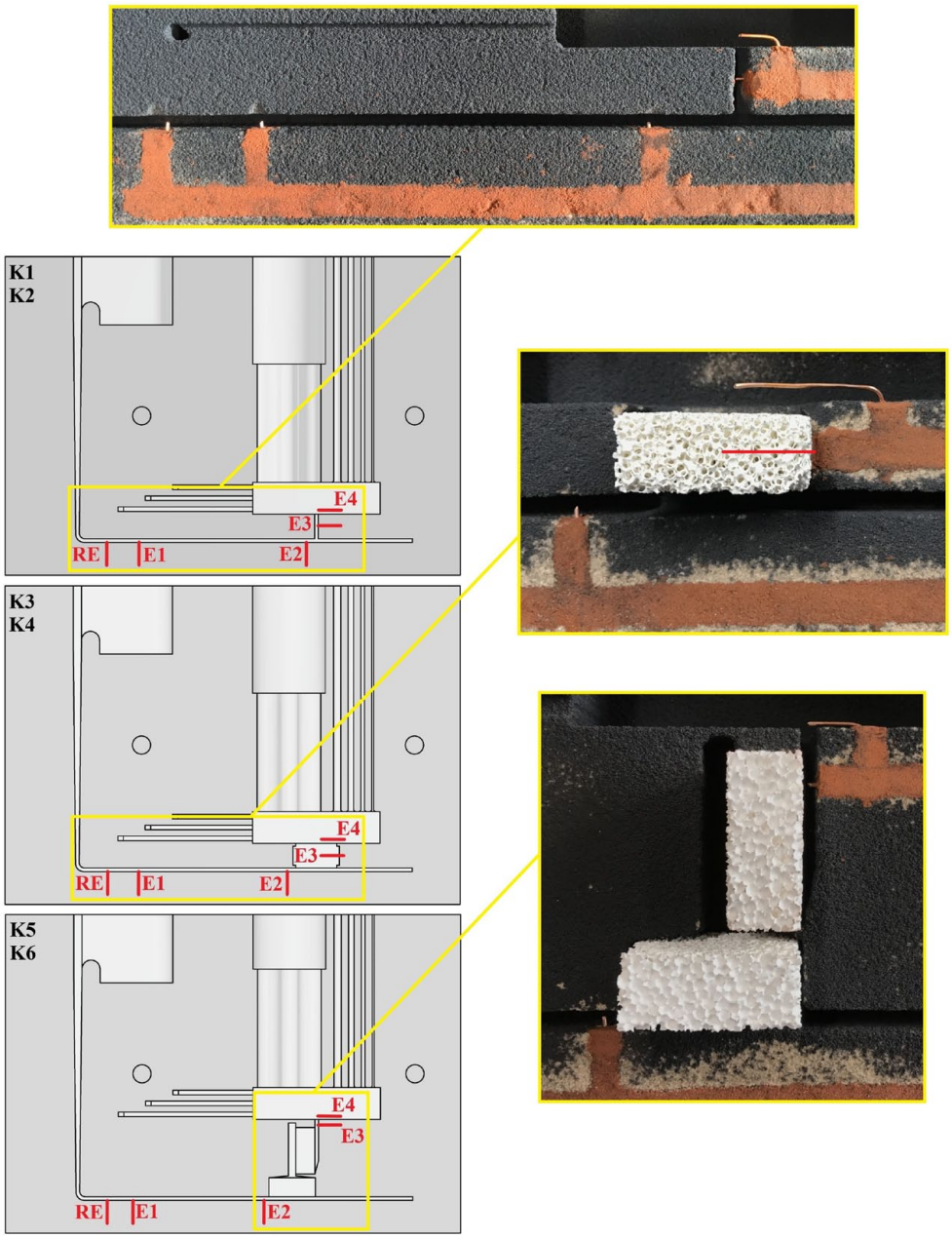

Fig. 3. Sensors placement in the molds

the E2 and E4 point during casting because a measurement error occurred. Designs 4 and 3 achieved the best results when the melt velocity decreased by approximately 85%, compared to the Design 1 at point E4. There was a 16% and 47% melt velocity reduction in Design 2 and 5, respectively, compared to Design 1.

In the simulations, the melt velocity was also measured at points which corresponded approximately to the location of the sensors in the molds. At E2 and E4 points. The results also shown the largest melt velocity reduction at point E4 in Designs 4 and 3, which achieved melt velocity reduction approximately 89% compared to Design 1. Compared to the reference gating system, melt velocity reductions of 35%, 63% and 74% were achieved in Design 2, Design 5 and Design 6.

A graph comparing the melt velocity values at points E2 and E4 measured by the sensors and simulations is shown in Fig. 4. From the graph, correlation of results between the values measured by sensors and simulations can be observed. Gate expansion in the Design 2 was not very effective in terms of melt velocity reduction. The use of a foam filter as in the Designs 3 and 4

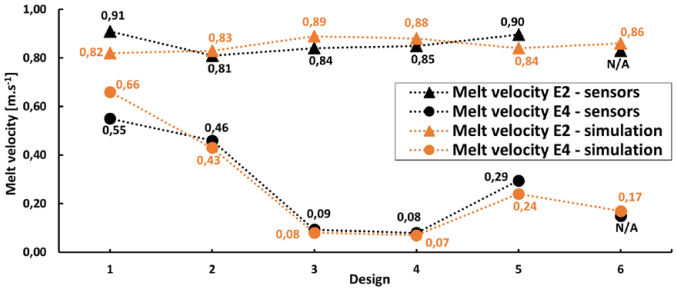

Fig. 4. Graph of melt velocity measured by sensors and simulation

ensured significant melt velocity reduction. The trident gate in the Designs 5 and 6 did not achieve the melt velocity reduction as expected, which may be attributed to the undersized dimensions of final gate element. The vortex element in the Design 6 at the end of the runner provided a reduction of melt velocity after gate in comparison to the Design 5.

3.2. Melt flow

The flow behind the gate was analysed by simulations and experiments using inspection fluid. In this work, the mold for the inspection fluid experiment was designed in a combination of a sand block and a PMMA plate attached to the front. The use of a sand mold allowed analysis of complicated geometries of the gating system elements. Use of a sand mold for the inspection fluid experiment was also advantageous in terms of maintaining similar conditions, such as friction, dynamic viscosity etc. The sand mold was made by patternless process method. After milling, the sand mold had to be treated with several layers of coating to prevent water seepage into the mold. White background was used to ensure contrast between the casted medium and the mold. Water at 52 ± 0.3°C was used for the experiment on the basis of similarity of Reynolds number between water and liquid aluminium alloy, which was explained in paper [18] and calculated by the same method, only for our gating dimensions. In order to maintain as much as possible the same conditions as for metal casting, it was casted from the same height and water level in the pouring basin was kept at the same level. Blue dye was added to the water to increase its visibility against the white mold background and orange dye was added with the intention of highlighting any turbulence in the inspection fluid. The fluid flow in the mold was captured on a GoPro HERO 11 camera in ultra-slow motion.

From the simulations and experiments with the inspection fluid, it could be seen that there was a high melt jump after gate in Design 1, fountain effect was formed, and the filling of the mold cavity was turbulent in the subsequent stages. In contrast, in Design 2, there was observed smaller melt jump after gate, but the flow was also turbulent and uncontrolled during filling. The foam filters in Design 3 and Design 4 provided significantly calmer filling conditions of the mold cavity without splashes,

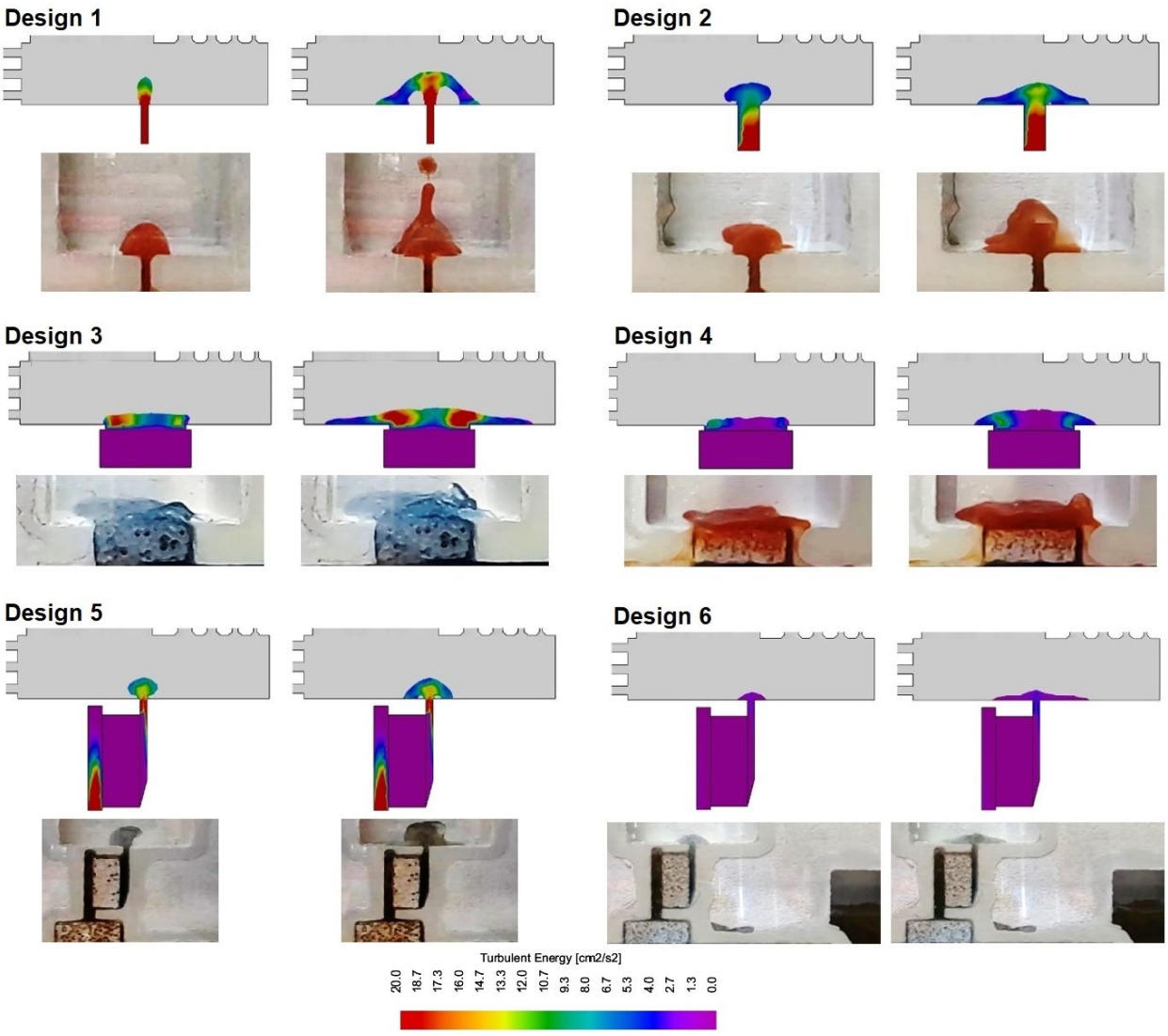

Fig. 5. Flow after gate analysed by simulation and experiment with inspection fluid

which was related to the significant reduction of the melt velocity. The higher density of the foam filter provided better results. Using trident gate in Design 5 and Design 6, the melt velocity was reduced compared to reference gating system. As a result, a splash reduction can be observed, but the filling of the mold cavity was turbulent. In the Design 6 with the vortex element at the end of the runner, a calmer filling conditions of the mold cavity can be observed compared to Design 5. By comparing the flow after gate using simulation and the experiment with the inspection fluid, it is possible to see a correlation between the obtained results. Water as a medium for the purpose of flow evaluation in the gating system seems to be suitable for comparison with the flow of the aluminium alloy. Fig. 5 shows results of simulations and experiments with inspection fluid.

3.3. Mechanical properties

Four specimens for tensile test and four specimens for notch toughness were taken from the casting as shown in Fig. 6. After the tensile tests, the elongation and the yield strength were evaluated. An Inspekt desk 50 kN was used for tensile test and the impact test was performed on PSW 30 machine. Mechanical properties were analysed after heat treatment of the specimens.

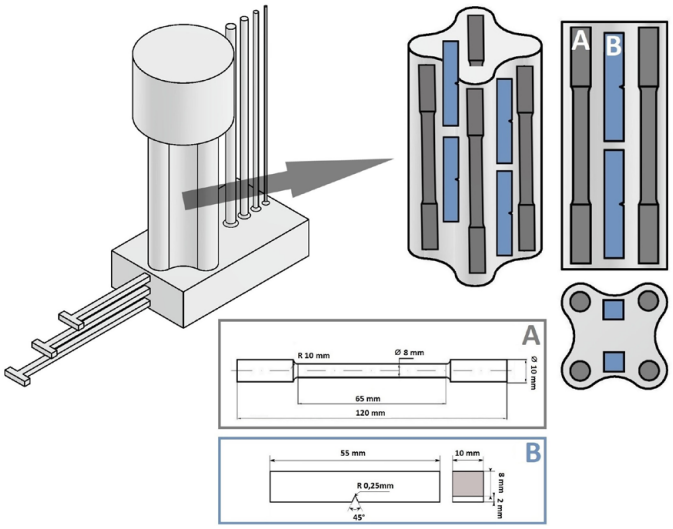

Fig. 6. Scheme of specimen placement for mechanical properties evaluation

Fig. 7 shows a graph with the measured average values of the mechanical properties depending on the design of the used gating system. It can be observed from the graph that the design of the used gating system did not have a significant effect on the notch toughness, except for Design 4, where there was an increase of 15% compared to Design 1. From the ultimate tensile strength and conventional yield strength results, it can be seen that the significant increase was achieved in the Designs 3 and Design 4 with foam filters, of witch better results was obtained by higher filter density. Compared to the reference gating system, improvement of about 18% in ultimate tensile strength and 70% in conventional yield strength were obtained in the Design 4. The ultimate tensile strength in Design 3 and Design 6 increased by 12% and 9%, respectively, and conventional yield strength by 58% and 43%, respectively, compared to Design 1. The Design 2 and Design 5 achieved approximately the same results, with ultimate tensile strength increase about by 5% and conventional yield strength increase about by 11%. The elongation decreased with increasing tensile strength. From the evaluation of the mechanical properties, it was possible to observe relationship between melt velocity, flow after gate and mechanical properties. With decreasing melt velocity after gate, a calmer filling of the mold cavity occurred. This may be related to the smaller amount of oxides solidified in the castings and the smaller amount of entrained air during turbulent filling of the mold cavity, resulting in better mechanical properties of the castings. In Design 4, the most significant reduction of melt velocity in the mold cavity and calm mold cavity filling conditions were achieved resulted to the significant increase of mechanical properties.

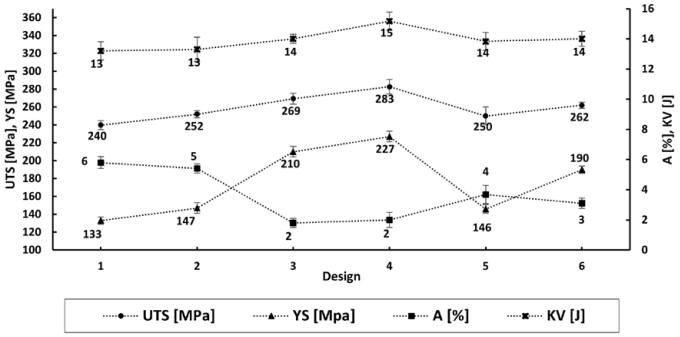

Fig. 7. Graph of mechanical properties

3.4. Microstructure

Samples for microstructure evaluation were taken from each casting from the same location. The microstructure of these samples was observed before heat treatment. Common preparation of aluminium alloy samples was used. An FEI Quanta FEG 450 auto-emission scanning electron microscope equipped with an Apollo X EDS analyser (EDAX) was used to observe the microstructure.

SEM images of the microstructure are shown in Fig. 8. The microstructure consists of α-phase and intermetallic phases excluded in the interdendritic spaces. The intermetallic phases are Al_2Cu in blocky form and Al_2Cu in a eutectic form, which has also been observed in several works [19,20]. Intermetallic iron phases have also been identified in the interdendritic spaces, as the used material contains about 0.11 wt.% Fe. In the microstructure, ferrous phases on the base of Al-Cu-Fe-Mn with plate morphology were observed, as in the work [21]. The microstructure assessment shown that the design of gating system was not affect the size of the α-phase and the size and distribution of the intermetallic phases.

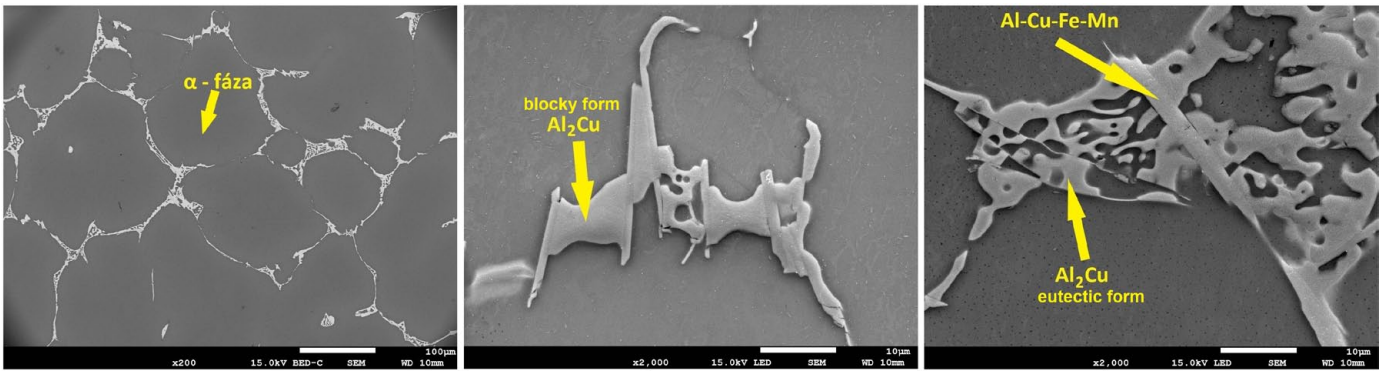

Fig. 8. SEM images of microstructure

4. Conclusions

Based on the experimental work can be stated following:

- The high melt velocity after gate caused a high melt jump and mountain flow effect in the mold cavity and turbulent flow in the later stages of the mold cavity filling.
- Experimental work has shown a correlation between melt velocity and the mechanical properties of castings. From the results obtained, it can be seen that by decreasing the melt velocity after gate the mechanical properties increased.
- The melt velocity measured during casting using sensors correlated with the results of melt velocity determined using simulations.
- The analysis of the flow using the simulation and using the inspection fluid experiment shown a correlation between the aluminium alloy and water during the mold cavity filling.
- The Design 4 achieved the most significant melt velocity reduction in the mold cavity, calm filling after gate and important increase of mechanical properties compared to the other gating system designs.

Acknowledgement

This article was produced within the UNIZA Grant System Project 01/2022 (17375) and VEGA 1/0241/23.

REFERENCES

[1] C.N. Nwambu, E.E. Nnuka, J.U. Odo, C.I. Nwoye, S.O. Nwakpa, Int. J. Eng. Sci. Invention Res. Dev. **3**, 20-24 (2014).

[2] H. Song, L. Zhang, F. Cao, X. Gu, J. Sun, Mater. Lett. **285**, (2021). DOI: https://doi.org/10.1016/j.matlet.2020.129089

[3] M.A. El-Sayed, PLoS One. **8**, (2016). DOI: https://doi.org/10.1371/journal.pone.0160633

[4] P. Lichý, M. Bajerová, I. Kroupová, T. Obzina, Mater. Tehnol. **54**, 263-265 (2020). DOI: https://doi.org/10.17222/mit.2019.147

[5] J. Campbell, Complete Casting Handbook, Oxford: Elsevier Ltd, 2015.

[6] J. Liu, Q. Wang, Y. Qi, Acta Mater. **164**, 673-682 (2019). DOI: https://doi.org/10.1016/j.actamat.2018.11.008

[7] M.M. Jalilvand, H. Saghafian, M. Divandari, M. Akbarifar, J. Magnes. Alloy **10**, 1704-1717 (2022). DOI: https://doi.org/10.1016/j.jma.2020.10.004

[8] R. Pastirčák, J. Ščury, J. Moravec, Arch. Foundry Eng. **17**, 103-106 (2017). DOI: https://doi.org/10.1515/afe-2017-0099

[9] G. Gyarmati, G. Fegyverneki, M. Tokár, T. Mende, Mater. Charact. **157**, (2019). DOI: https://doi.org/10.1016/j.matchar.2019.109925

[10] K. Metzloff, K. Mageza, D. Sekotlong, Int. J. Met. **14**, 610-621 (2020). DOI: https://doi.org/10.1007/s40962-020-00471-w

[11] A. Remišová, M. Brůna, Arch. Foundry Eng. **19**, 55-60 (2019). DOI: https://doi.org/10.24425/afe.2019.129630

[12] R. Dojka, J. Jezierski, J. Campbell, J. Mater. Eng. Perform. **27**, 5152-5163 (2018). DOI: https://doi.org/10.1007/s11665-018-3497-1

[13] H. Yavuz, A. Kara, H.E. Çubuklusu, Ö.B. Çe, U. Aybarç, J. Achiev. Mater. Manuf. Eng. **75**, 71-77 (2016). DOI: https://doi.org/10.5604/17348412.1228381

[14] H.Y. Hwang, C.H. Nam, Y.S. Choi, J.H. Hong, X. Sun, China Foundry **14**, 216-225 (2017). DOI: https://doi.org/10.1007/s41230-017-6108-0

[15] F.Y. Hsu, C.L. Li, J. Campbell, Key Eng. **573**, 19-29 (2013). DOI: https://doi.org/10.4028/www.scientific.net/KEM.573.19

[16] J. Jezierski, R. Dojka, K. Janerka, Metals **27**, 5152-5163 (2018). DOI: https://doi.org/10.1007/s11665-018-3497-1

[17] M. Papanikolaou, E. Pagone, M. Jolly, K. Salonitis, Metals **10**, (2020). DOI: https://doi.org/10.3390/met10010068

[18] C. Bate, P. King, J. Sim, G. Manogharan, Materials **16**, (2023). DOI: https://doi.org/10.3390/ma16020756

[19] M. Zamani, S. Toschi, A. Morri, L. Ceschini, S. Seifeddine, J. Therm. Anal. Calorim. **139**, 3427-3440 (2020). DOI: https://doi.org/10.1007/s10973-019-08702-x

[20] A. Lombardi, W. Mu, C. Ravindran, N. Dogan, M. Barati, J. Alloys Compd. **747**, 131-139 (2018). DOI: https://doi.org/10.1016/j.jallcom.2018.02.329

[21] B. Andilab, C. Ravindran, N. Dogan, A. Lombardi, G. Byczynski, Mater. Charact. **159**, (2020). DOI: https://doi.org/10.1016/j.matchar.2019.110064